Journal of ELECTRONIC MATERIALS, Vol. 37, No. 6, 2008
DOI: 10.1007/s11664-008-0411-x
© 2008 TMS

Formation of Intermetallic Compounds Between Liquid Sn and Various $CuNi_x$ Metallizations

V. VUORINEN,[1,2] H. YU,[1] T. LAURILA,[1] and J.K. KIVILAHTI[1]

1.—Laboratory of Electronics Production Technology, Helsinki University of Technology, PL 3000 (Otakaari 7A), Helsinki 02015 HUT, Finland. 2.—e-mail: Vesa.Vuorinen@tkk.fi

Interfacial reactions between liquid Sn and various Cu-Ni alloy metallizations as well as the subsequent phase transformations during the cooling were investigated with an emphasis on the microstructures of the reaction zones. It was found that the extent of the microstructurally complex reaction layer (during reflow at 240°C) does not depend linearly on the Ni content of the alloy metallization. On the contrary, when Cu is alloyed with Ni, the rate of thickness change of the total reaction layer first increases and reaches a maximum at a composition of about 10 at.% Ni. The reaction layer is composed of a relatively uniform continuous $(Cu,Ni)_6Sn_5$ reaction layer (a uniphase layer) next to the NiCu metallizations and is followed by the two-phase solidification structures between the single-phase layer and Sn matrix. The thickness of the two-phase layer, where the intermetallic tubes and fibers have grown from the continuous interfacial $(Cu,Ni)_6Sn_5$ layer, varies with the Ni-to-Cu ratio of the alloy metallization. In order to explain the formation mechanism of the reaction layers and their observed kinetics, the phase equilibria in the Sn-rich side of the SnCuNi system at 240°C were evaluated thermodynamically utilizing the available data, and the results of the Sn/Cu_xNi_{1-x} diffusion couple experiments. With the help of the assessed data, one can also evaluate the minimum Cu content of Sn-(Ag)-Cu solder, at which $(Ni,Cu)_3Sn_4$ transforms into $(Cu,Ni)_6Sn_5$, as a function of temperature and the composition of the liquid solders.

Key words: Intermetallic formation, soldering, lead-free, solidification, kinetics, metastable solubility, reliability, phase diagram

INTRODUCTION

Manufacturing of novel portable electronic devices with new functions and higher performance is increasing concerns about the reliability of such products. Additional requirements are set by the implementation of lead-free materials, which demand careful consideration of compatibility between dissimilar materials for attaining high yield and reliability of lead-free equipment with an economically acceptable level of reliability testing. Therefore, especially under mechanical shock loading, where the strain-rate hardening of the solder material forces cracks to propagate in the intermetallic layers, the role of interfacial intermetallic reactions as well as microstructural evolution in solder interconnections becomes more prominent.[1–3]

The formation of intermetallic compounds (IMCs) in the solid state (during high-temperature annealing or thermal cycling) has been reported extensively in numerous publications, where it has been stated that solid-state diffusion is the rate-limiting step in IMC formation.[4–12] On the other hand, during reflow soldering, metal atoms from the components and/or printed circuit boards (PCBs) dissolve rapidly into the liquid solder and the IMC formation occurs very quickly. However, what really

(Received November 16, 2007; accepted February 13, 2008; published online March 14, 2008)

happens within the first few seconds of soldering is not yet known unambiguously. For example, a detailed study of the microstructures of the regions next to the Sn/Cu interface revealed numerous tubes and bundles of Cu_6Sn_5 fibers inside the solder matrix, the formation of which has not been clarified.[13]

In a few recent publications[14–20] the formation of intermetallic layers between Cu-bearing lead-free solders and a Ni substrate or between Ni-bearing lead-free solders and a Cu substrate have been explained by making use of the diagram proposed by Lin et al.[21] On the other hand, Hsu et al.[22] and Wang and Liu[23] used an earlier preliminary version of the Sn-Cu-Ni isothermal section[24,25] to explain the formation of $(Cu,Ni)_6Sn_5$ in soldering reactions between Cu-alloyed Sn-Ag solders and a Ni substrate as well as in the Ni/Sn-3.5Ag/Cu sandwich structure. However, the authors did not consider either the supersaturation of the solder with dissolved Cu and Ni atoms or the existence of the metastable solubility limit. In addition, the effect of temperature change on local equilibria at the interfaces was not taken into account. The published results show slightly different values related to the minimum amount of Cu in Sn-based solders which is required to change the primary intermetallic compound from $(Ni,Cu)_3Sn_4$ to $(Cu,Ni)_6Sn_5$ between the solder and Ni metallization.[14–23] For example, Alam et al. presented that after 20 min annealing of Sn-3.5Ag-0.5Cu (wt.%) on Ni/Au metallization at 240°C the Cu content of the liquid has decreased to 0.2 wt.%, and that was the reason why $(Ni,Cu)_3Sn_4$ started to form between Ni and $(Cu,Ni)_6Sn_5$.[26] Hsu et al. annealed the binary liquid SnCu solders on Ni/Ti thin-film metallization at 250°C for different periods of time up to 20 min.[22] They reported that already after 30 s a layer of $(Ni,Cu)_3Sn_4$ was formed at the interface when using Sn-0.6Cu (wt.%) solder and that the higher Cu-contents resulted in the formation of $(Cu,Ni)_6Sn_5$.[22] Wu et al. reported the formation of $(Cu,Ni)_6Sn_5$ in the reaction between Ni/Au metallization and Sn-3.0Ag-0.5Cu wt.% solder when a peak reflow temperature of 250°C and time of 75 s were used.[16] Ho et al. studied the reactions between Ni and Sn-Ag-Cu solders at 250°C.[15] The Ag content was fixed at 3.9 wt.%, Cu content varied between 0.0 wt.% and 3.0 wt.%, and the soldering times used were from 10 min to 25 h. They found out that when the Cu content was 0.2 wt.% or less, $(Ni,Cu)_3Sn_4$ was the only phase to form. On the other hand, when the Cu content was 0.6 wt.% or higher, $(Cu,Ni)_6Sn_5$ was the only reaction product. When the Cu content was 0.4 wt.%, continuous $(Ni,Cu)_3Sn_4$ was formed with a small amount of discontinuous $(Cu,Ni)_6Sn_5$ particles on the top. With Sn-3.9Ag-0.5Cu (wt.%) both intermetallics were formed as continuous layers, but the $(Ni,Cu)_3Sn_4$ was very thin.[15] Chen et al. studied interfacial reactions between binary Sn-Cu solders and Ni at 250°C for 10 min and 25 h.[14] The Cu contents used were 0.2 wt.%, 0.4 wt.%, 0.7 wt.%, and 1 wt.%. The results were similar to those of Ho et al.[15] With Sn-0.2Cu (wt.%) solder $(Ni,Cu)_3Sn_4$ and with Sn-0.7Cu (wt.%) or Sn-1.0Cu (wt.%) $(Cu,Ni)_6Sn_5$ were the only phases to form. When Sn-0.4Cu was used as the solder, both intermetallic layers were formed.[14]

The purpose of the present article is to study experimentally and theoretically the formation of interfacial reaction layers and related microstructures in solder interconnections. Since the most potential Pb-free solders are high-Sn alloys and Cu and Ni are generally used in metallizations, especially in high-density assemblies, it is of interest to study the ternary Sn-Cu-Ni system. The phase relations in the Sn-Cu-Ni system has been studied experimentally at soldering temperatures by Obernsdorf[13] as well as by Lin et al.[21] Their phase diagrams differ to some degree with regard to the solubility of a third element (i.e., Cu or Ni) to the binary intermetallics as well as to the existence of ternary intermetallic compound 44Sn27Cu29Ni (at.%).[13] These issues were taken into account during the modeling of the high-Sn section of the Sn-Cu-Ni system at typical reflow temperatures.[27] The interfacial reactions are studied experimentally by employing the Sn/CuNi, SnCu/Ni, and SnNi/Cu reaction (diffusion) couples. Especially, the effect of Ni content in the Cu metallization on the interfacial reactions with liquid Sn is studied in detail. Further, based on the evaluated thermodynamic data, the interfacial reactions between Cu-bearing lead-free solders and Ni metallizations, as reported also by various authors, are discussed, by taking into account the supersaturation of the liquid solder, metastable solubility limits, and the effects of temperature on the local equilibria. Finally, the basis for evaluating the effect of additional elements on the interfacial reactions between liquid Cu-containing solder and Ni is provided.

MATERIALS AND METHODS

Cu-Ni substrate alloys with the following Ni contents: 2.5, 5, 7.5, 10, 12.5, 15, 25, 37.5, 50, and 75 (at.%), were prepared by melting pure (99.99%) metals in quartz tubes under vacuum and annealing them more than 50°C above the liquidus of each alloy for 15 min. The alloys were cold-rolled to a thickness of 0.5 mm and then annealed at 700°C for 8 h to achieve uniform composition. Subsequently, the strips were cut into $5 \times 20\ mm^2$ strips, the surfaces of which were ground and polished. The reaction couple experiments were carried out in a stainless-steel crucible by immersing the Cu, Ni, and CuNi alloy strips into a high-purity (99.99%) liquid (T = 240°C) Sn bath. To obtain additional data needed for evaluating the phase equilibria, several ternary Sn-Cu-Ni alloys and diffusion couples were annealed at temperatures from 125°C to 320°C for different periods of time (up to 13,000 h). After the annealing and standard metallographic

preparation, the cross sections of the liquid/solid reaction couples were examined with optical microscopy (Olympus B20) and scanning electron microscopy (SEM)/energy-dispersive spectroscopy (EDS) technique (Jeol 6335F/Oxford INCA). The thermodynamic description of the Sn-rich part of the Sn-Cu-Ni system was carried out by using the binary systems Ni-Cu,[28] Sn-Cu,[29] and Sn-Ni[30] as well as the published experimental isothermal sections at 235°C and 240°C.[13,21]

On the Phase Equilibria in the Sn-Cu-X System

Thermodynamics of materials provides fundamental information both on the stability of phases and on the driving forces for chemical reactions and diffusion processes, even though the complete phase equilibrium is hardly ever met in electronics applications. However, stable or metastable local equilibria are generally attained at interfaces, which provides a feasible method—together with kinetic information—for analyzing the interfacial reactions in solder interconnection systems. This approach, which makes use of the tie lines of binary and ternary phase diagrams as well as the stability diagrams, is becoming increasingly important when studying interconnections under continuous microstructural evolution. For this purpose the special concept of the local nominal composition (LNC) in the effective joint region can be utilized.[31]

The phase equilibria in solder or solder-substrate systems (as in any system) are computed by first summing up all the Gibbs (free) energies of individual phases (i.e., solutions and compounds) and then minimizing—according to the second law of thermodynamics—at constant temperature and pressure the total Gibbs energy of the n-component system:

$$G_{\text{tot}} = \sum_{\phi}\sum_{i}(G_i^{\phi} n_i^{\phi}) = \sum_{\phi} y^{\phi} \sum_{i=1}^{n}\left(x_i G_i^0 + RT\sum_{i}^{n} x_i \ln x_i + G_m^E\right), \tag{1}$$

where y is the relative amount of a phase ϕ, and x_i is the mole fraction of component i in the system.[32] The parameters G_i^0 in Eq. 1 represent the partial molar Gibbs energies or chemical potentials of the pure components and are taken from the Scientific Group Thermodata Europe (SGTE) databank[28] and from the literature.[33] G_m^E is the excess molar Gibbs energy taking into account the interactions of the constituents in all the phases to be modeled.

The two-phase equilibrium between liquid Sn rich solution and the intermetallic compound $(Cu,X)_6Sn_5$ is of great technological interest in solder-substrate systems. It can be computed thermodynamically from the assessment of the ternary systems. Even though more complicated models are used in the calculations in this article, simple thermodynamic models can be used to show how the calculation is performed in principle and what are the most significant parameters. The lattice ratio of Cu_6Sn_5 is practically constant. If we assume that the third element, say Ni atoms, occupies the Cu sublattice sites randomly, the ternary intermetallic compound can be regarded as a binary regular solution phase $(Cu,Ni)_6Sn_5$ composed of Cu_6Sn_5 and Ni_6Sn_5 components. Then the molar Gibbs energy of the $(Cu,Ni)_6Sn_5$ (=IMC) will be

$$G_m^{\text{IMC}} = (1-y)G^0_{\text{Cu6Sn5}} + yG^0_{\text{Ni6Sn5}} + aRT[y\ln y + (1-y)\ln(1-y)] + ay(1-y)I^{\text{IMC}}_{\text{Cu,Ni}}, \tag{2}$$

where y is the site fraction of Ni atoms in the Cu sublattice, G^0_{Cu6Sn5} is the standard molar Gibbs energy of Cu_6Sn_5, G^0_{Ni6Sn5} is the standard molar Gibbs energy of the hypothetical component Ni_6Sn_5, a (= $x_{\text{Cu}} + x_{\text{Ni}} \equiv 6/11$) is the number of substitutional sites in the Cu sublattice and $I^{\text{IMC}}_{\text{Cu,Ni}}$ is the interaction parameter between Cu and Ni in the IMC, which can depend on composition and temperature. The chemical potentials of Cu_6Sn_5 and Ni_6Sn_5 components in $(Cu,Ni)_6Sn_5$ are therefore presented as

$$\mu_{\text{Cu6Sn5}} = \mu^0_{\text{Cu6Sn5}} + aRT\ln(1-y) + aI^{\text{IMC}}_{\text{Cu,Ni}}y^2 \quad \text{and} \quad \mu_{\text{Ni6Sn5}} = \mu^0_{\text{Ni6Sn5}} + aRT\ln y + aI^{\text{IMC}}_{\text{Cu,Ni}}(1-y)^2. \tag{3}$$

The condition for the two-phase equilibrium between Sn-rich liquid and $(Cu,Ni)_6Sn_5$ will be

$$a\mu^L_{\text{Cu}} + (1-a)\mu^L_{\text{Sn}} = \mu_{\text{Cu6Sn5}} \quad \text{and} \quad a\mu^L_{\text{Ni}} + (1-a)\mu^L_{\text{Sn}} = \mu_{\text{Ni6Sn5}} \tag{4}$$

Because the solubility of both Cu and Ni in liquid Sn is limited, Sn-rich liquid is dilute ($x^L_{\text{Sn}} \approx 1$, $1-x^L_{\text{Cu}} \approx 1$, $1-x^L_{\text{Ni}} \approx 1$) and can be described by a regular solution model, and therefore the chemical potentials in Eq. 4 can be calculated as

$$\mu^L_{\text{Cu}} \approx \mu^{0,L}_{\text{Cu}} + RT\ln x^L_{\text{Cu}} + I^L_{\text{Sn,Cu}} \quad \text{and} \quad \mu^L_{\text{Ni}} \approx \mu^{0,L}_{\text{Ni}} + RT\ln x^L_{\text{Ni}} + I^L_{\text{Sn,Ni}}, \tag{5}$$

where $\mu^{0,L}_{\text{Cu}}$ and $\mu^{0,L}_{\text{Ni}}$ are the standard chemical potential of pure liquid Cu and Ni, $I^L_{\text{Sn,Cu}}$ and $I^L_{\text{Sn,Ni}}$ are the interaction parameters in liquid. By assuming that all the interaction parameters are constant the Eqs. 2–5 will lead to the distribution coefficient of Ni between liquid solder and Cu_6Sn_5

$$k^{L/\text{IMC}}_{\text{Ni}} = \frac{x^L_{\text{Ni}}/x^L_{\text{Cu}}}{x^{\text{IMC}}_{\text{Ni}}/x^{\text{IMC}}_{\text{Cu}}} = \frac{(1-y)x^L_{\text{Ni}}}{yx^L_{\text{Cu}}} = \exp\left(\frac{Q}{aRT}\right) \text{ where}$$
$$Q \approx (G^0_{\text{Cu6Sn5}} - G^0_{\text{Ni6Sn5}}) - a\left(\mu^{0,L}_{\text{Cu}} - \mu^{0,L}_{\text{Ni}}\right) - \left(I^L_{\text{Sn,Cu}} - I^L_{\text{Sn,Ni}}\right) + aI^{\text{IMC}}_{\text{Cu,Ni}}(2y-1). \tag{6}$$

The values of the variables in the equations given above can be obtained by fitting the regular solution models (both $(Cu,Ni)_6Sn_5$ and liquid) with the calculated Gibbs energies in certain composition and temperature ranges, by using the thermodynamic assessment of the Sn-Cu-Ni system. The detailed information can be found in Ref. [27]

As stated above, the local equilibrium condition is generally fulfilled in soldering systems. This means that, although the chemical potentials (or activities) of the components have the same value at the interface (local equilibrium), there are activity gradients in the adjoining phases. These gradients provide the driving force for the formation and growth (diffusion) of the various phases. Therefore, even if detailed kinetic data are not available, the impossible sequences of reaction products can be ruled out by utilizing the mass balance requirement together with the fundamental condition that no atom can diffuse intrinsically against its own activity gradient.[34] These can, in turn, be calculated from the assessed thermodynamic data.

RESULTS

When studying the formation of intermetallic compounds with the help of Sn/Cu-Ni_x alloy diffusion couples, microstructurally and kinetically interesting behavior was observed. Figure 1 shows how the average thickness of the reaction layer varies as a function of the Ni content of the binary substrate alloy immersed in molten Sn for 10 min at 240°C. The alloys with Ni content of about 10 at.% exhibit the fastest reaction rate, which is many times higher than those obtained with pure Cu or Ni. Similar results were obtained when the $(Cu,Ni)_6Sn_5$ layer was formed in the reaction between Sn-rich solders and Sn-Cu-Ni alloys.[35] In addition, the reaction zone is composed of two different morphologies. A continuous uniform layer of the intermetallic compound (uniphase) can be observed in contact with the Cu-Ni alloy. On the top of the uniphase layer there is a two-phase layer containing IMC needles and fibers, which are embedded in the Sn matrix. The thickness of the two-phase layer is strongly dependent on the composition of the alloy (i.e., the Cu-to-Ni ratio). In the samples with a high reaction rate the reaction layer is mainly composed of the two-phase layer and the thickness varies considerably.

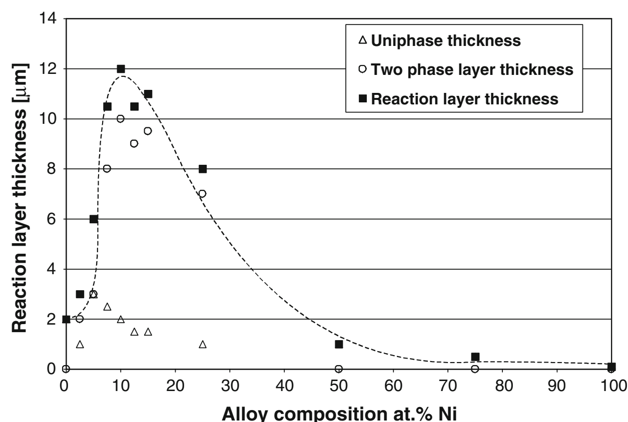

Fig. 1. Reaction layer thickness of different Sn/Cu-Ni diffusion couples at 240°C.

Figure 2a–d shows the typical microstructures of the reaction layers when high-purity Cu, Cu-Ni alloys with two different Ni contents (2.5 at.% and 15 at.%), and high-purity Ni were immersed in molten Sn for 10 min at 240°C. In the case of the 97.5Cu-2.5Ni alloy (Fig. 2b), the thickness of the intermetallic layer is relatively small but the morphology differs slightly from that normally observed in the Sn-Cu system (see Fig. 2a). As can be seen from Fig. 2d, the thickness of the $(Ni,Cu)_3Sn_4$ is very small. On the other hand, in the case of the 85Cu-15Ni alloy the thickness of the layer is remarkably large and the morphology of the intermetallic layer differs from the typical scallop-like appearance of Cu_6Sn_5. The layer clearly exhibits two different morphologies: a uniphase layer next to the substrate followed by a two-phase zone. More-detailed SEM observations revealed that the second layer is composed of IMC tubes embedded in the Sn matrix (see Fig. 3, which is from the same sample as in Fig. 2c but more heavily etched). The corresponding microstructures containing the same features, i.e., hexagonal tubes or whiskers filled with

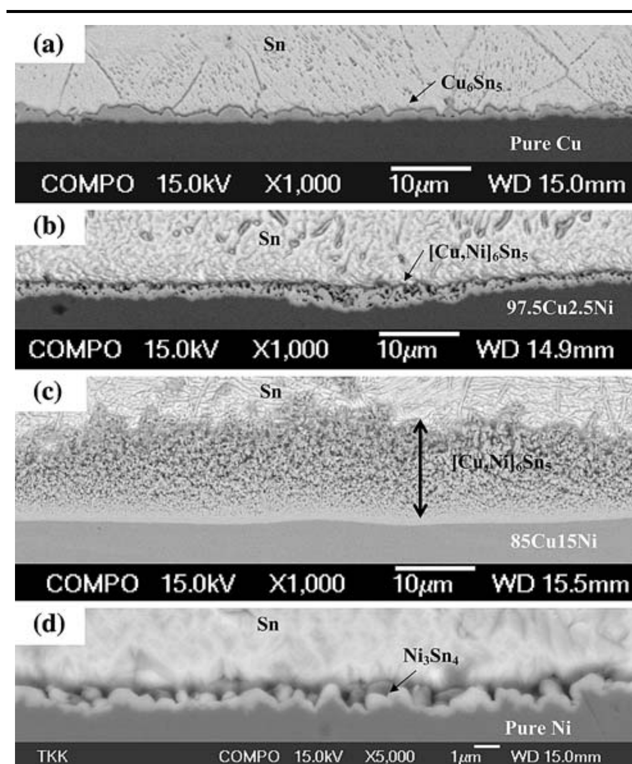

Fig. 2. (a) Pure Cu/Sn, (b) 97.5Cu-2.5Ni/Sn, (c) 85Cu-15Ni/Sn, and (d) pure Ni/Sn (higher magnification) diffusion couples annealed at 240°C for 10 min.

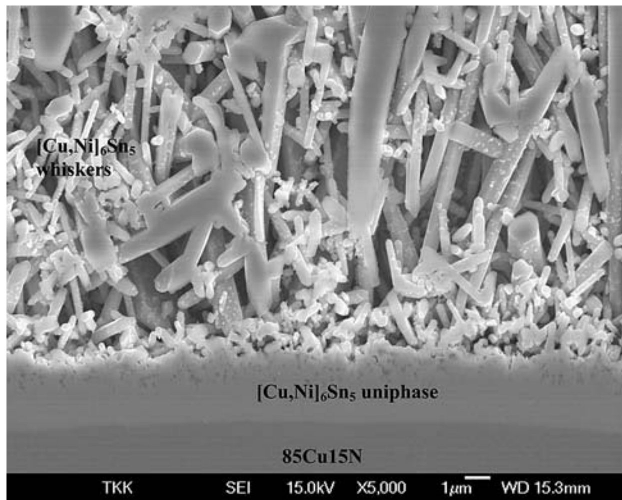

Fig. 3. 85Cu-15Ni/Sn diffusion couple annealed at 240°C for 10 min. More heavily etched than Fig. 2c.

solder alloy, have also been reported elsewhere.[13] The two-phase structure can be seen more clearly in Fig. 4b, where the sample was annealed at 240°C for 60 min. The thickness of the uniphase layer is the same after 10 min and 60 min immersion. However, the thickness of the two-phase layer has increased markedly. On the other hand, when the sample was annealed for only 1 min at 240°C (see Fig. 4a), the uniphase is clearly observable but the two-phase layer is very thin.

The chemical microanalyses of the Sn/Cu-Ni_x diffusion couples indicates that the intermetallic phase (both the uniphase and the IMC needles in the two-phase layer) is $(Cu,Ni)_6Sn_5$. The structure of this phase corresponds to the binary Cu_6Sn_5 compound where Ni atoms have substituted some of the Cu atoms, as also reported by other authors.[15,36–38] There are some variations in the Cu-to-Ni ratio of the intermetallic compounds with the different substrates studied. Typically, the Cu-to-Ni ratio was close to (or slightly more Ni than) that of the base alloy. The existence of the $(Cu,Ni)_6Sn_5$ compound and solubility even up to 50 at.% of Ni in the Cu sublattice at 220°C has also been reported.[7] Moreover, a ternary 44Sn27Cu29Ni phase has also been identified at 240°C.[13] However, the growth kinetics of the stable ternary 44Sn27Cu29Ni compound is very slow, and therefore during the relatively short periods of time used in soldering only metastable $(Cu,Ni)_6Sn_5$ compounds of different Cu-to-Ni ratios can form.

On the basis of these results, together with the results from the long-term diffusion couple experiments, as well as other published information,[7,13,21,35,39] a metastable isothermal section (Fig. 5) of the Sn-Cu-Ni system can be constructed at 240°C. This metastable diagram does not include either the solid miscibility gap in the binary Cu-Ni system or the ternary 44Sn27Cu29Ni compound (τ) observed at this temperature. The position of the possible τ-phase is marked with a gray dot (Fig. 5).

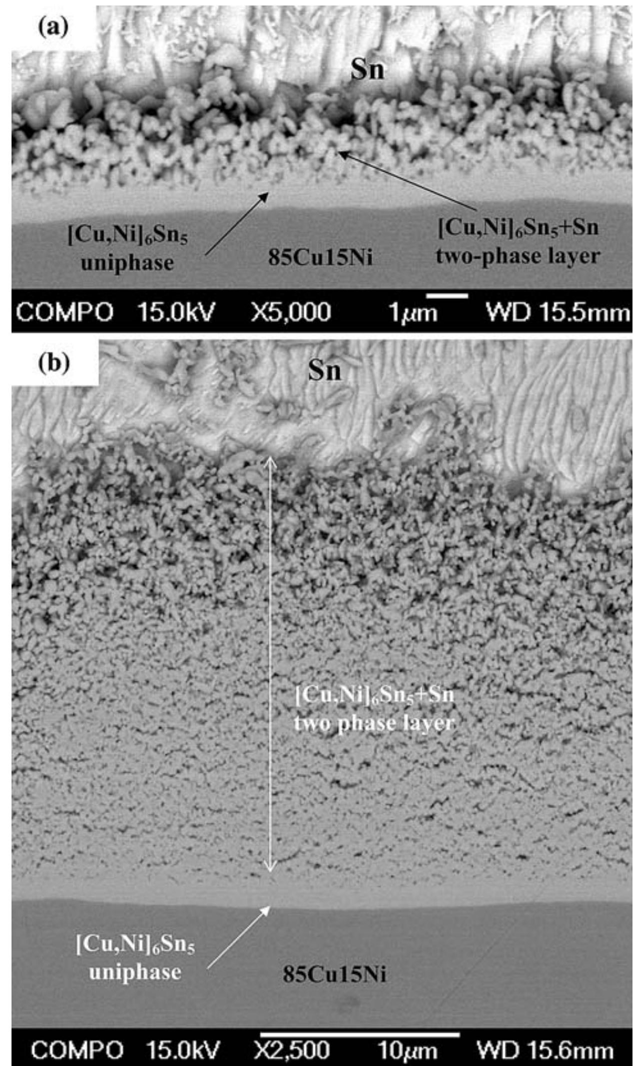

Fig. 4. 85Cu-15Ni/Sn diffusion couple annealed at 240°C for (a) 1 min and (b) 60 min.

The phase equilibria in the CuNi-rich side of the system at temperatures below 300°C are not well known because of the extremely low diffusion and reaction kinetics.[7,13] The phase separation between Cu_3Sn and Ni_3Sn is observed at higher temperatures[40,41] and the thermodynamic assessment shows that the high-temperature phases can be stable at these temperatures in the ternary region.[27,42] However, these phases/compounds were not observed in the diffusion couples, except when very long (>1000 h) annealing times were used. Therefore, the phase equilibria in this area are drawn with dashed lines. The $(Cu,Ni)_6Sn_5$ and $(Ni,Cu)_3Sn_4$ intermetallics can be considered as line compounds, since they exist in narrow composition ranges in the binary systems. The results presented by Lin et al. indicate that the solubilities of Cu in Ni_3Sn_4 and Ni_3Sn_2 are 10 at.% and 36.5 at.%, respectively.[21] On the other hand, Oberndorf reported smaller solubility values of 7 at.% and 11 at.% to 17 at.%.[13]

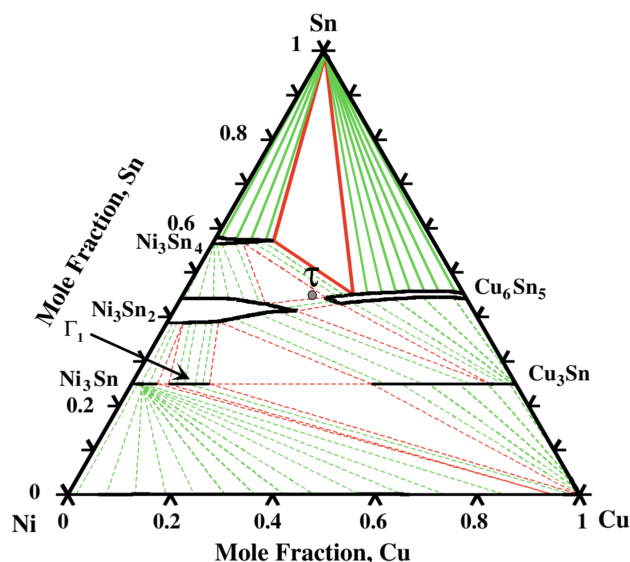

Fig. 5. Calculated metastable equilibria of the Sn-Cu-Ni system at 240°C. The position of the possible τ-phase is marked with a gray dot. The phase equilibria in the CuNi-rich side of the system at low temperatures are not well known and are therefore drawn with dashed lines.

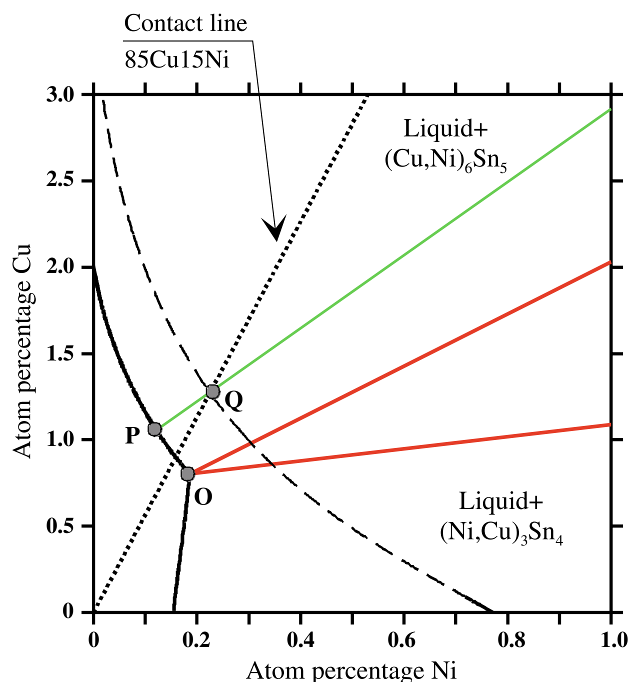

Fig. 6. Sn-rich corner of the optimised metastable phase diagram at 240°C. The contact line (from pure Sn to the original 85Cu-15Ni alloy) is drawn with a dotted line. Metastable solubility is shown with a dashed curve.

DISCUSSION

Differing markedly from solid-state diffusion couples, in which the growth of an intermetallic layer is slow, the formation of reaction layers can be very rapid if one of the contact materials is in a liquid state. In the latter case the dissolution rate of a solid metal in liquid solder has a significant effect on the growth kinetics of intermetallic compounds. In some liquid solder/conductor systems the intermetallic compound layers have been observed to build up within seconds,[43] and thus the nucleation and growth of intermetallic compounds has to occur by some other mechanism than those that are operative in solid-state diffusion.

On the basis of the results presented above it seems evident that intermetallic compounds form by chemical reaction between dissolved metal atoms and the most active component atoms of solder (the highest Gibbs energy of formation) as well as by solidification from the supersaturated liquid. The reactions occur on substrate (conductor) metal, which provides a catalytic surface. After the initial formation of the intermetallic reaction layer from locally supersaturated liquid further growth can occur during the cooling, as observed in the Au-Sn system.[44]

Phase Equilibria and Reactions in the Sn-Cu-Ni System

To explain the kinetic and microstructural observations presented above detailed information about the local phase equilibria, especially close to the Sn-rich corner of the diagram (see Fig. 6), is required. The one-phase liquid region (on the bottom left) is bordered by the two-phase regions $[(Ni,Cu)_3Sn_4 + Liq]$ and $[(Cu,Ni)_6Sn_5 + Liq]$. The two-phase boundaries intersect at the apex of the three-phase triangle denoted by the point O. The position of this point as a function of temperature is especially important and will be discussed in detail later on. During the short soldering period, the composition of the molten solder changes along the contact line from the liquid Sn to the original 85Cu-15Ni alloy shown in Fig. 6. The dashed curve cutting the contact line at the point Q indicates the metastable solubilities of Cu-Ni alloys in liquid Sn. This metastable curve was calculated by suspending all the intermetallic phases as discussed in Ref. 44. Hence, the composition of the liquid in local metastable equilibrium with solid Cu-Ni metallization is determined by the metastable solubilities of the Cu and Ni atoms. These solubility values, which are determined by mutual interactions of the atoms in the liquid, also establish the maximum driving forces for the formation of solid $(Cu,Ni)_6Sn_5$ or $(Ni,Cu)_3Sn_4$ intermetallics, as well as have significant effect on the mobilities of the Cu and Ni atoms in the liquid solder. Therefore, the thickness of the intermetallic compound(s) formed within the first few seconds is dependent on the metastable solubilities and the mobilities of the atoms in the liquid.

When the local metastable solubility denoted by the intersection point Q (in Fig. 6, see Table I) is reached at the interface, the solid $(Cu,Ni)_6Sn_5$ compound layer will nucleate on the Cu/Ni

Table I. Calculated Compositions of Points O, P, and Q at 240°C

Points (see Fig. 6)	Cu Content (at.%)	Ni Content (at.%)
Point O	0.80	0.19
Point P	1.05	0.12
Point Q	1.30	0.23

metallization. The composition of the $(Cu,Ni)_6Sn_5$ reaction layer and that of the liquid (point P in Fig. 6, see Table I) in local equilibrium with the reaction layer can be read from the ends of the tie line passing the point Q. Since the diffusion of Cu and Ni atoms in the solid reaction layer, i.e., the uniphase layer, is very slow, the thickness of the initially formed $(Cu,Ni)_6Sn_5$ layer is controlled by the amounts of Cu and Ni atoms available on the liquid side of the interface.

In order to explain the increase in the thickness of the intermetallic layer when Cu is alloyed with Ni, the effect on the dissolution rate and solubility must be considered. As can be seen from Fig. 6, according to the thermodynamic assessment both the stable and metastable solubilities are reduced with the addition of Ni to Cu. In order to obtain data about the dissolution rate, a few experiments were performed which compared the amount (thickness) of dissolved metallization between pure Cu and Cu-12.5Ni as a function of time. The immersion times in liquid Sn (T = 240°C) that were used were 1 min, 10 min, and 30 min. As can be seen from Fig. 7, the thickness of the Cu_6Sn_5 layer is almost the same in all samples with pure Cu (left), but changes drastically when the Cu-12.5Ni alloy is used (right). So even after 30 min the thickness of the pure Cu_6Sn_5 is only about 1 μm, while that of the $(Cu,Ni)_6Sn_5$ is almost 10 μm. On the other hand, as much as about 200 μm of Cu has dissolved from Cu to liquid Sn during the 30 min of immersion (see Fig. 8a). It is to be noted that a relatively large volume of liquid Sn (~200 g) was used in order to prevent saturation. Figure 9 shows the measured (see Fig. 8b) average dissolution rates of pure Cu and Cu-12.5Ni as a function of time. Although the IMC thickness is much greater when using the

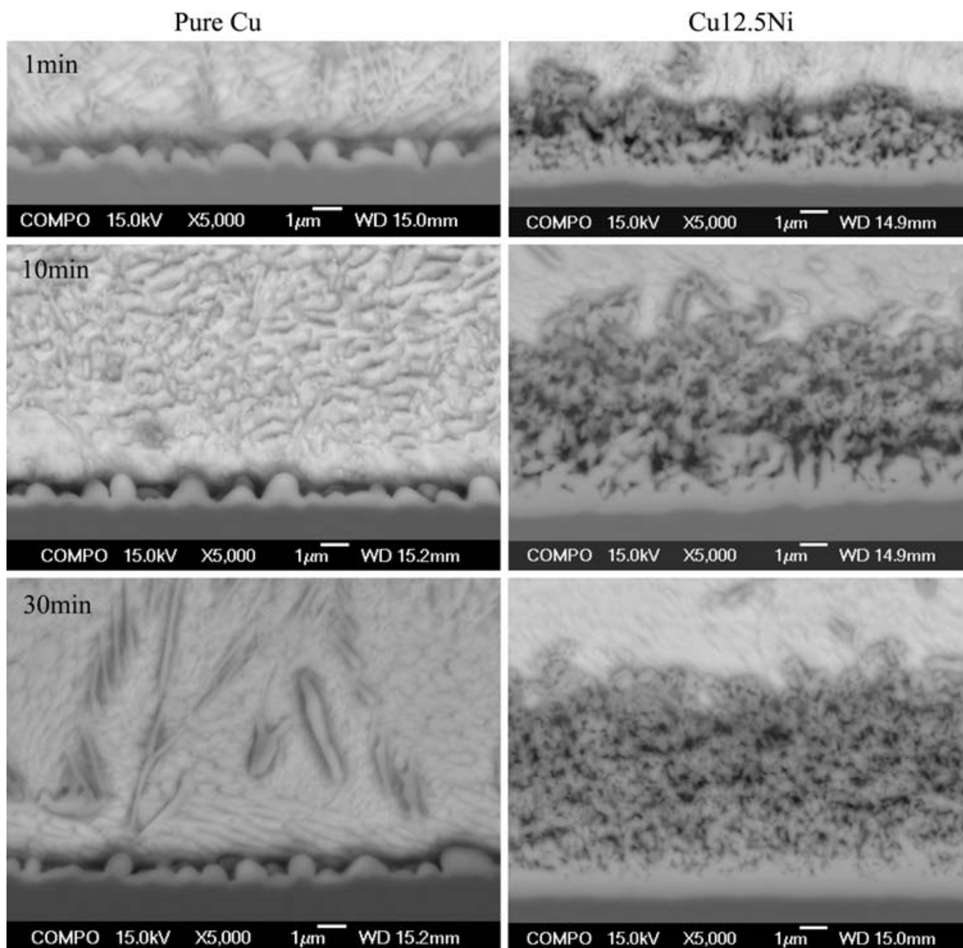

Fig. 7. Intermetallic layers in pure Cu/Sn (left) and 87.5Cu-12.5Ni/Sn (right) diffusion couples annealed at 240°C for 1 min (top), 10 min (middle), and 30 min (bottom).

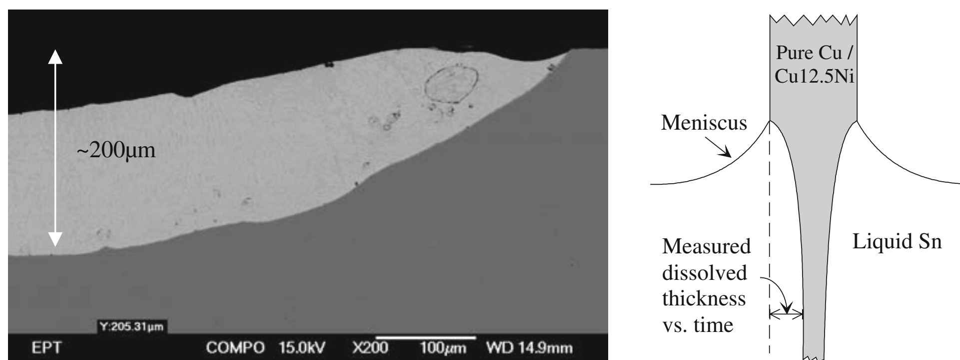

Fig. 8. (a) Amount of dissolved Cu after 30 min immersion in Sn at 240°C (tilted 90 degrees clockwise), and (b) schematic representation of the measurement setup.

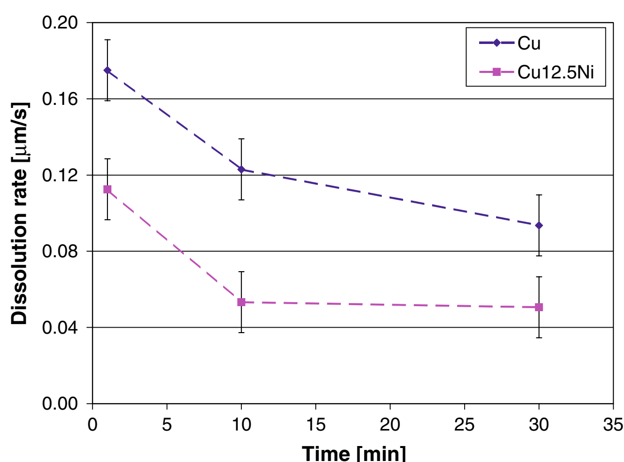

Fig. 9. Measured average dissolution rates of pure Cu and Cu-12.5Ni in liquid Sn at 240°C as a function of time.

Cu-12.5Ni alloy, the dissolution rate is clearly lower than that of pure Cu. The effect of saturation can be seen from Fig. 10 (Cu-12.5Ni/Sn at 240°C for 30 min), where the reaction layer is considerably higher at the solder meniscus than further from the surface of the bath.

During the cooling of the liquid, the reactions depend primarily on the composition of the liquid next to the $(Cu,Ni)_6Sn_5$ uniphase layer. For example, in the diffusion couple between the liquid Sn and 85Cu-15Ni metallization the primary $(Cu,Ni)_6Sn_5$ crystals nucleate on and grow from the $(Cu,Ni)_6Sn_5$/liquid interface, generating long intermetallic needles or solder-filled tubes, which constitute, together with the Sn matrix, the two-phase reaction layer as seen in Fig. 3. Using the optimized thermodynamic data, the evolution of different phases in the alloy system with composition P (see Fig. 6) can be evaluated as a function of temperature. The results of the calculations presented in Fig. 11a–d show that, due to the low solubility of Ni in liquid Sn, the solidification starts with the formation of $(Cu,Ni)_6Sn_5$ at about 231°C and then continues by simultaneous formation of $(Cu,Ni)_6Sn_5$ and bct-Sn [Liq + $(Cu,Ni)_6Sn_5$ $\rightarrow$ bct-Sn + $(Cu,Ni)_6Sn_5$] between 229°C and the eutectic temperature of the binary Cu-Sn system, as can be seen from Fig. 11a. It is also to be noted that, as the solubility of Ni in solid Sn is very small and the Ni content of the liquid approaches zero during cooling, all the dissolved Ni atoms should be incorporated into $(Cu,Ni)_6Sn_5$. On the other hand, if the Ni content of the supersaturated liquid beside the IMC is different from that indicated by point P, the solidification path will change as will be discussed later on.

It is obvious that, the longer the CuNi metallization is immersed in the liquid, the more Cu and Ni atoms can dissolve. Therefore, the two-phase reaction layer is much thicker with longer immersion times. On the other hand, when the contact line (for example 25Cu-75Ni) passes the point O from the

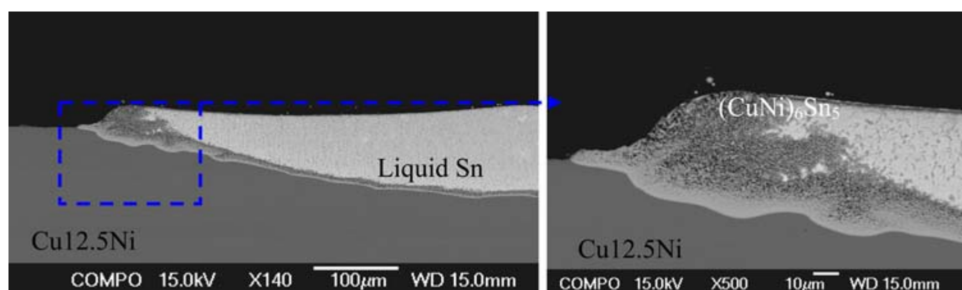

Fig. 10. Effect of saturation on the IMC thickness at the meniscus. Cu-12.5Ni/Sn at 240°C for 30 min.

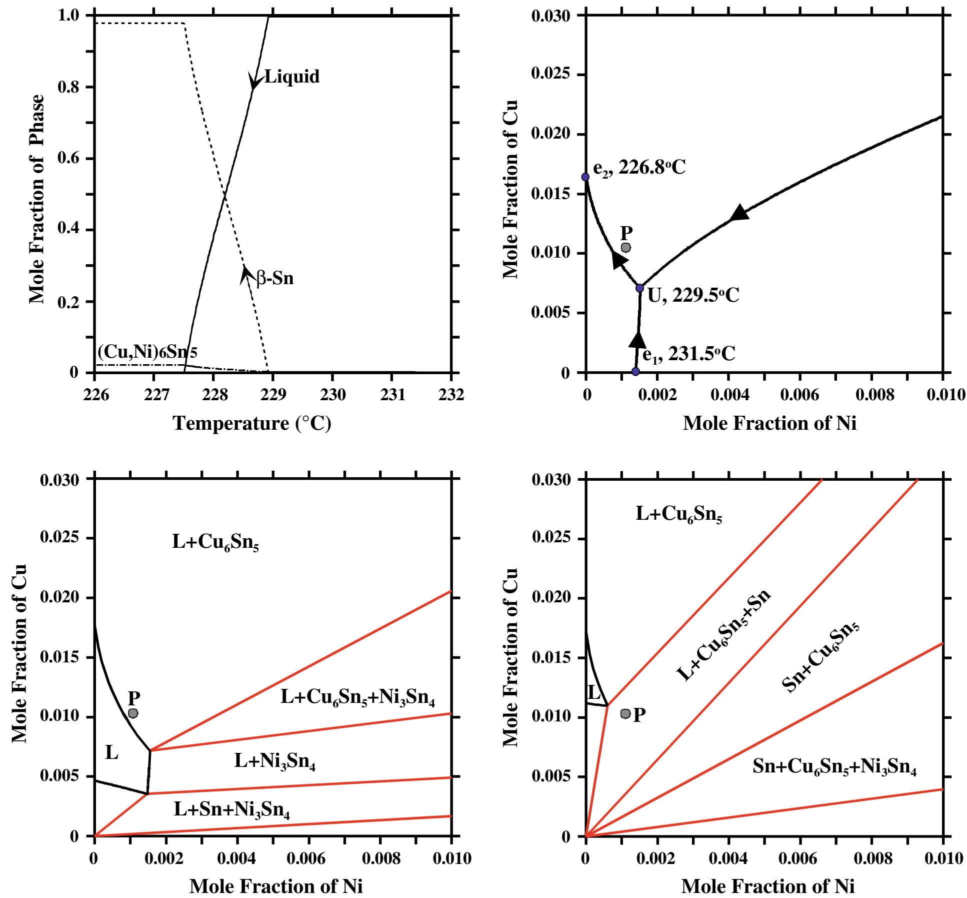

Fig. 11. (a) Relative amount of phases during cooling when the nominal composition is Sn-1.05Cu-0.12Ni (at.%), i.e., point P in Fig. 6, (b) liquidus projection from the Sn-rich corner of the Sn-Cu-Ni system, and (c,d) isothermal sections from the Sn-rich corner of the Sn-Cu-Ni system one degree above (230.5°C) as well as below (228.5°C) the ternary point U (L + Ni_3Sn_4 → Cu_6Sn_5 + Sn), respectively.

right-hand side (Fig. 6), the Ni-to-Cu ratio is high enough for the formation of a thin $(Ni,Cu)_3Sn_4$ layer, instead of $(Cu,Ni)_6Sn_5$. Another parameter that has a significant effect on both the morphology and the thickness of the intermetallic reaction layer is the cooling rate. The results presented above were obtained from samples where the cooling rate was high, i.e., the metal strips were removed from the solder bath and only a small amount of liquid Sn, containing some dissolved Cu and Ni, was left on the surface of the strips. Therefore another set of experiments was carried out in which the metal strip was allowed to cool down in the solidifying Sn bath. Two different relatively slow cooling rates (after 10 min immersion) from 240°C down to 225°C were used (4°C/min and 1.3°C/min). It is to be noted that because of the slow cooling rates the total times above liquidus were about 12 min and 16 min, respectively, and therefore the thickness of the reaction layers is not comparable to the results presented above.

As can be seen from Fig. 12, the interfacial microstructure after slow cooling (1.3°C/min) is very uneven. On the Sn side, close to the reaction layer, the microstructure is composed of eutectic-type regions between Sn crystals. When comparing the microstructures between pure Cu and Cu-12.5 Ni after 10 min immersion in liquid Sn at 240°C and cooling at the rate of 4°C/min (i.e., total liquid time about 12 min), it can clearly be seen (see Fig. 13a–f) that there are marked differences. First, the eutectic-type structure (IMC crystals embedded in Sn matrix) can be observed further from the interface with pure Cu than Cu-12.5Ni. In order for this to be seen more clearly, a dashed red line is drawn in Fig 13a and b. Secondly, the amount of eutectic structure near the interface is higher with pure Cu than with Cu-12.5Ni (see Fig. 13c and d). These facts support the findings above that (i) the dissolution rate of pure Cu is higher than that of Cu12.5Ni and (ii) Cu concentration evens out more rapidly in the liquid Sn when Ni is absent. Finally, as expected, the total reaction layer thickness is considerably higher with Cu-12.5Ni (see Fig. 13e and f). On the contrary, the uniphase layer has about the same thickness in both samples. On the basis of these results the following conclusions can be drawn (i) due to the strong mutual interaction between Cu, Ni, and Sn in the liquid the dissolving Cu and Ni atoms remain close to the solid-liquid

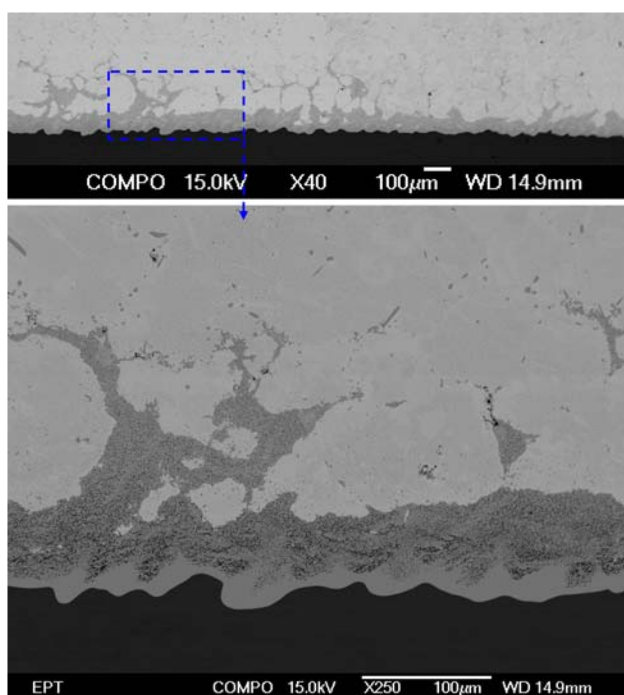

Fig. 12. Interfacial microstructures from Cu-12.5Ni/Sn diffusion couple, slow cooling (1.3°C/min).

interface and this enables the formation of a thick two-phase reaction layer and decreases the driving force for dissolution because of supersaturation, (ii) with the pure Cu/Sn reaction couple the Cu atoms migrate further away from the original interface and the local supersaturation is not high enough for the formation of the thick two-phase layer or for the dissolution to slow down significantly. This, in turn, leads to the higher amount of IMC precipitates in front of the much thinner two-phase layer as can be seen from Fig. 13a, c, and e.

Critical Cu Content in Reactions Between Sn-rich Solders and Ni Metallizations

The thermodynamic-kinetic approach can also be used for predicting the intermetallic reaction products in Cu-containing lead-free solders with Ni metallizations. Figure 14 shows the Sn-rich corner of the isothermal section of the Sn-Cu-Ni phase diagram at 250°C. For the sake of simplicity it is presented here in weight percentages and the tie lines are left out. If the Cu content of the solder is less than ~0.4 wt.% (indicated with a), the contact line intersects the metastable solubility curve in the Liq + $(Ni,Cu)_3Sn_4$ two-phase region (indicated with b) and therefore $(Ni,Cu)_3Sn_4$ nucleates at the Ni/solder interface. However, if the Cu concentration is larger than 0.6 wt.% (indicated with c), the intersection point d is in the Liq + $(Cu,Ni)_6Sn_5$ two-phase region and so $(Cu,Ni)_6Sn_5$ must be the first intermetallic phase to form. When the Cu content in Sn-rich solder is near 0.5 wt.% as Ni atoms start to dissolve into solder containing Cu, the supersaturation causes the liquid to become local equilibrium with both $(Cu,Ni)_6Sn_5$ and $(Ni,Cu)_3Sn_4$ (i.e., metastable solubility line inside the three-phase triangle) and thermodynamically either of these can form at the interface. However, when the temperature is not constant (as in soldering) the phase equilibria will change as a function of temperature. These changes can be examined with the help of Fig. 15, in which the apex of the three-phase triangle, i.e., the critical Cu content of the solder, is presented as a function of temperature. The dark gray (below invariant temperature) and light gray areas (below liquidus lines) in Fig. 15 indicate the solid and solid + liquid areas, respectively; above (to the left of) the dotted line the primary intermetallic is $(Cu,Ni)_6Sn_5$ and below (to the right of) it the primary intermetallic is $(Ni,Cu)_3Sn_4$. The circles [$(Cu,Ni)_6Sn_5$] and squares [$(Ni,Cu)_3Sn_4$] represent the experimental results performed to verify and reoptimize the movement of the apex of the three-phase triangle (point O, at Fig. 14) as a function of temperature. It is clear that the reoptimized data (dashed line) is more consistent with the experimental results than the original data (dotted line,[27]), especially at temperatures below 280°C. For example, when the Cu content of the solder is 0.4 wt.% and the peak reflow temperature is 250°C, $(Ni,Cu)_3Sn_4$ will form first, but when the temperature decreases below 240°C $(Cu,Ni)_6Sn_5$ becomes in local equilibrium with the solder. This can also be seen from Fig. 16, which shows how the primary intermetallic (with constant Cu content) is changed from $(Cu,Ni)_6Sn_5$ to $(Ni,Cu)_3Sn_4$ when the temperature is increased. It is to be noted that, owing to the large amount of solder, alloy changes in nominal composition (Cu content) are not expected. It is interesting to note that the IMC thickness is clearly reduced when it is changed from $(Cu,Ni)_6Sn_5$ to $(Ni,Cu)_3Sn_4$, even when the temperature is increased. On the other hand, it seems that the interface between Ni and IMC is more uneven when the composition is near to the equilibrium curve. Therefore it can be concluded that the effect of temperature on the critical Cu composition is significant and thus it is now possible to explain the $(Cu,Ni)_6Sn_5$ precipitates on the top of the $(Ni,Cu)_3Sn_4$ observed in Refs. [14,15,18,19] when the Cu content of the Sn-Ag-Cu solder was 0.4 wt.%. As can be seen from Fig. 17, a similar trend can also be observed if the temperature is kept constant (T = 240°C) and the Cu content is reduced.

Effect of Alloying Elements on the Critical Cu Content

The addition of other alloying elements may change the critical Cu content for $(Cu,Ni)_6Sn_5$ formation. Ho et al.[15] suggested that the existence of Ag in the Sn-Ag-Cu solder does not have any effect, since it dissolves in neither $(Ni,Cu)_3Sn_4$ nor $(Cu,Ni)_6Sn_5$. This is only partly true, because the

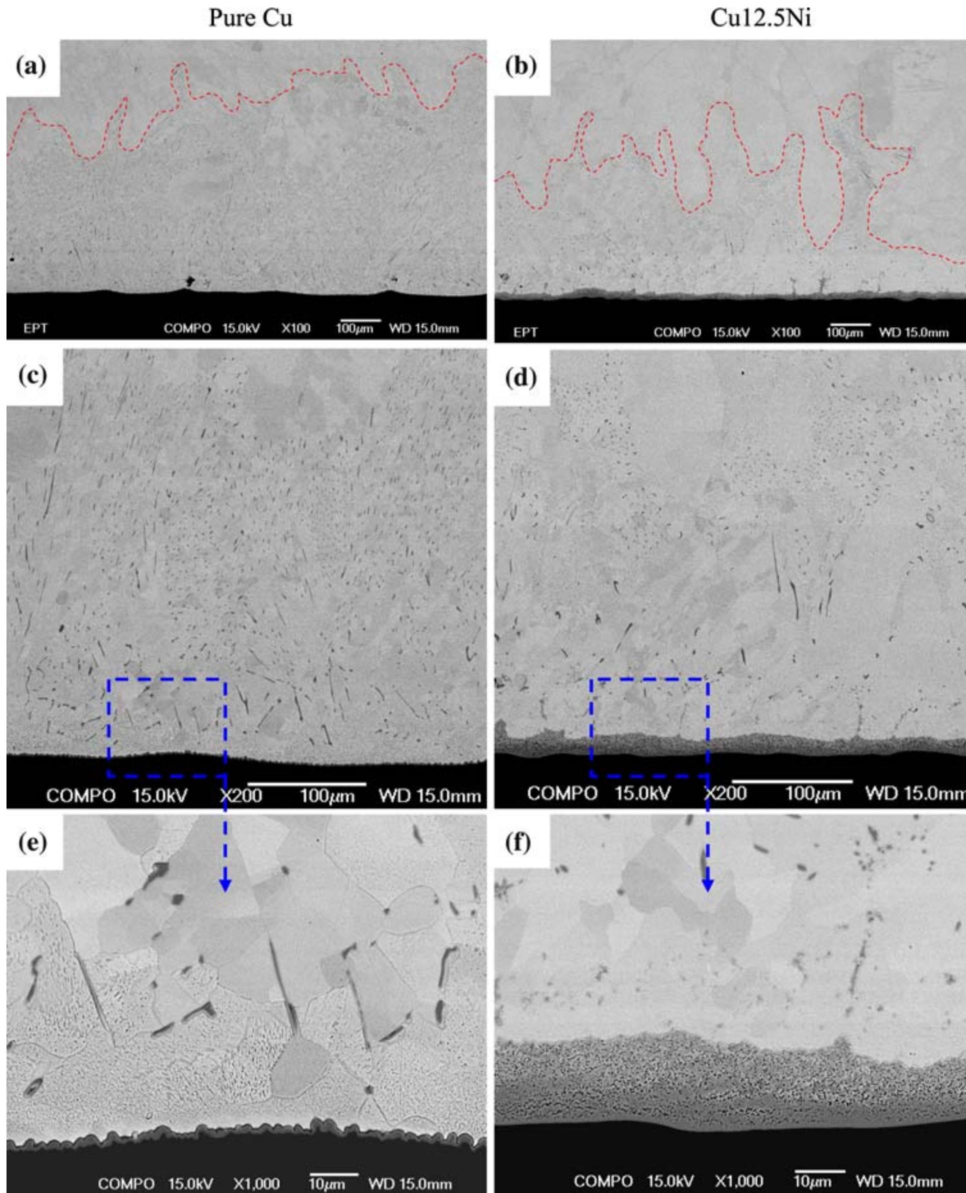

Fig. 13. Interfacial microstructure after 10 min at 240°C and slow (4°C/min) cooling of the pure Cu/Sn (left) and Cu-12.5Ni/Sn (right) diffusion couples.

activities of the elements, not only in the compounds themselves but also in a liquid in (local) equilibrium with the compounds, determine the relative stabilities of $(Ni,Cu)_3Sn_4$ and $(Cu,Ni)_6Sn_5$. In order to demonstrate this, we collected the liquid parameters available in the literature for the Sn-Cu-Ni-Ag system and calculated the critical Cu content. As shown in Fig. 18, the critical Cu content decreases from ~0.43 wt.% to ~0.36 wt.% Cu with the addition of Ag to the liquid solder. Bismuth is another much-used alloying element in lead-free solders. If we add, say, 3 wt.% Bi to the liquid alloy the critical composition of the liquid further decreases to ~0.32 wt.% Cu. This means that both Ag and Bi should reduce the critical Cu content and their combined effect could be up to 25% in commercial lead-free alloys generally used in industry, even though they do not dissolve in either of the compounds. As for other alloying elements, their influences on the activities of components in both liquid and intermetallic compounds should be taken into account; this is an interesting subject for future studies.

CONCLUSIONS

Interfacial reactions between liquid Sn (as well as Cu or Ni-alloyed Sn-Ag solders) and Cu, Ni, or various Cu-Ni alloy metallizations were rationalized with the help of microstructural characterization

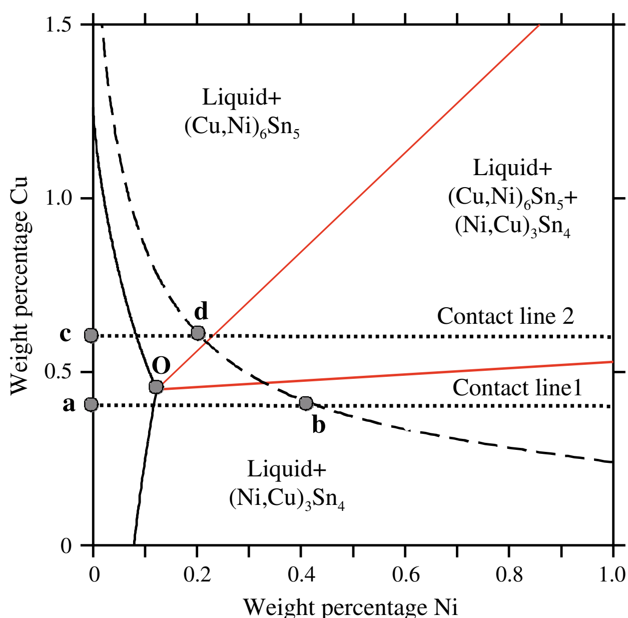

Fig. 14. Sn-rich corner of the optimized metastable phase diagram at 240°C.

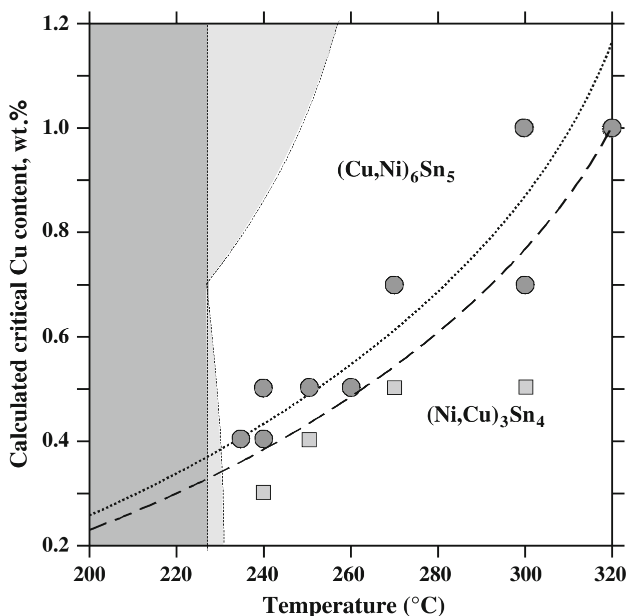

Fig. 15. Calculated critical Cu content in liquid Sn to change the interfacial reaction product from $(Ni,Cu)_3Sn_4$ to $(Cu,Ni)_6Sn_5$, as a function of temperature together with the experimental points. Original data[42] with dotted line and reoptimized data with dashed line.

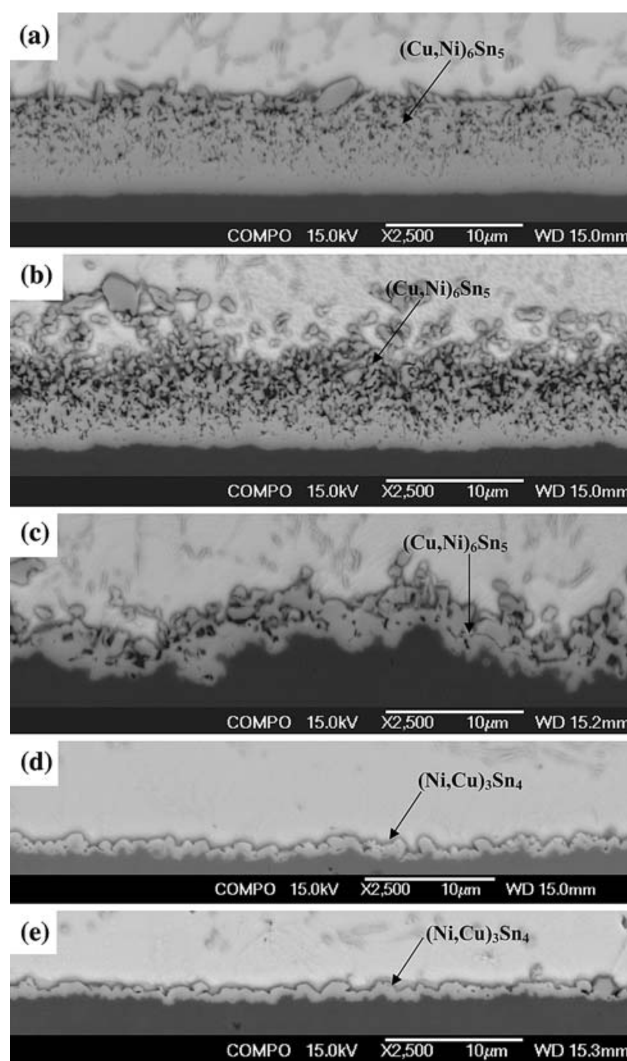

Fig. 16. Sn + 0.5 wt.% Cu/Ni diffusion couples annealed at (a) 240°C, (b) 250°C, (c) 260°C, (d) 270°C, and (e) 300°C for 60 min.

techniques and thermodynamic modeling of the interconnection system in order to have a better understanding of the formation of complex reaction zones in solder/conductor systems. The following results were obtained: (i) firstly, it was discovered that the formation of the reaction layers during soldering at 240°C does not depend linearly on the Ni content of the Cu-Ni alloy metallization. Instead, when Cu is alloyed with Ni, the rate of growth of the thickness of the total reaction layer increases, reaching its maximum at a composition of about 10 at.% Ni. With higher Ni contents, the thickness of the reaction layer starts to decrease and attains a very low value with pure Ni. The reaction layer is composed of a relatively uniform $(Cu,Ni)_6Sn_5$ reaction layer (or uniphase layer) next to the Cu_xNi_{1-x} metallizations and a microstructurally more complex two- or three-phase layer between the uniphase layer and the Sn matrix. It is argued that because of the strong interaction between Ni and Sn atoms the presence of Ni slows down the migration of Cu and Ni atoms in the liquid. This is consistent with the experimental results about the effect of Ni on the solubility rates and leads to the situation where both dissolving components (Cu and Ni) stay relatively close to the solid/liquid interface instead of diffusing further into the liquid as in the case of the pure Cu/Sn system. Therefore, the liquid near the

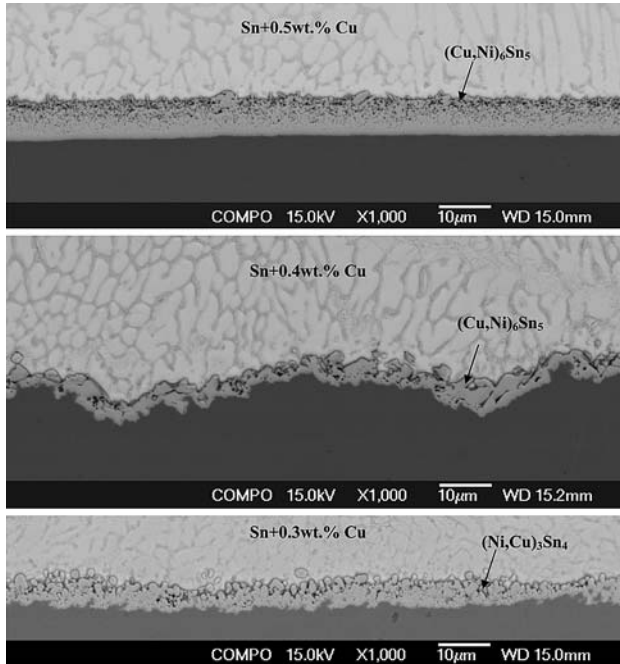

Fig. 17. Sn + (a) 0.5 wt.% Cu, (b) 0.4 wt.% Cu, and (c) 0.3 wt.% Cu/Ni diffusion couples annealed at 240°C for 60 min.

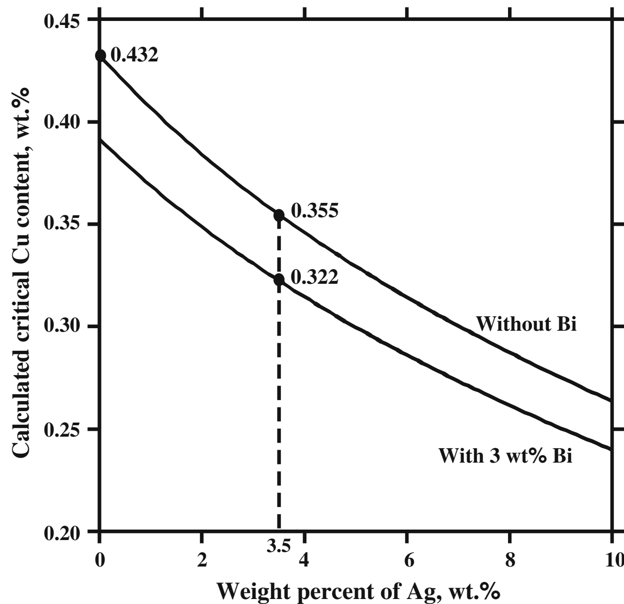

Fig. 18. Effect of alloying Ag and Bi to Sn on the critical Cu content at T = 250°C.

solid base metal becomes highly supersaturated with Ni and Cu, which in turn leads to the formation of a thick two-phase solidification structure, as observed experimentally. (ii) Secondly, with the help of the assessed data the critical Cu content of liquid Sn-Cu solder was evaluated. With a Cu content less than about 0.4 wt.% at 250°C, $(Ni,Cu)_3Sn_4$ is thermodynamically more stable than $(Cu,Ni)_6Sn_5$. (iii) Thirdly, it was shown that the critical Cu content is not only temperature dependent but is also strongly affected by alloying elements, such as Ag or Bi, that do not even dissolve in the intermetallic compounds.

REFERENCES

1. J. Kivilahti, *IEEE T. Compon. Pack. T. B.* 18, 326 (1995).
2. J.K. Kivilahti, *JOM-J. Min. Met. Mat. S.* 54, 52 (2002).
3. T.T. Mattila and J.K. Kivilahti, *J. Electron. Mater.* 34, 969 (2005).
4. K.N. Tu, *Acta Metall. Mater.* 21, 347 (1973).
5. K.N. Tu and R. Thompson, *Acta Metall. Mater.* 30, 947 (1982).
6. K.N. Tu, *Mater. Chem. Phys.* 46, 217 (1996).
7. M. Oh (Doctoral thesis, Leigh University, 1994).
8. H. Bhedwar, K. Ray, S. Kulkarni, and V. Balasubramanian, *Scripta Metall. Mater.* 6, 919 (1972).
9. M. Onishi and H. Fujibuchi, *Trans. Jpn. Inst. Met.* 16, 539 (1975).
10. Z. Mei, A. Sunwoo, and J. Morris, *Metall. Trans. A* 23A, 857 (1992).
11. S. Bader, W. Gust, and H. Hieber, *Acta Metall. Mater.* 43, 329 (1995).
12. J. Haimovich, *Weld. J.* 68, 102 (1989).
13. P. Oberndorff (Doctoral thesis, Eindhoven University of Technology, 2001).
14. W.T. Chen, C.E. Ho, and C.R. Kao, *J. Mater. Res.* 17, 263 (2002).
15. C.E. Ho, R.Y. Tsai, Y.L. Lin, and C.R. Kao, *J. Electron. Mater.* 31, 584 (2002).
16. P.-L. Wu, M.-K. Huang, C. Lee, and S.-R. Tzan, *J. Electron. Mater.* 33, 157 (2004).
17. J.Y. Tsai, Y.C. Hu, C.M. Tsai, and C.R. Kao, *J. Electron. Mater.* 32, 1203 (2003).
18. C.E. Ho, Y.L. Lin, S.C. Yang, C.R. Kao, and D.S. Jiang, *J. Electron. Mater.* 35, 1017 (2006).
19. C.E. Ho, Y.L. Lin, S.C. Yang, and C.R. Kao, *Proceedings of 10th International Symposium on Advanced Packaging Materials, IEEE* (2005).
20. W.C. Luo, C.E. Ho, J.Y. Tsai, Y.L. Lin, and C.R. Kao, *Mater. Sci. Eng. A Struct.* 396, 385 (2005).
21. C.-H. Lin, S.-W. Chen, and C.-H. Wang, *J. Electron. Mater.* 31, 907 (2002).
22. S.C. Hsu, S.J. Wang, and C.Y. Liu, *J. Electron. Mater.* 32, 1214 (2003).
23. S.J. Wang and C.Y. Liu, *J. Electron. Mater.* 32, 1303 (2003).
24. "IPMA" *The Thermodynamic Databank for Interconnection and Packaging Materials* (Helsinki University of Technology, Helsinki, 2006).
25. K. Zeng, V. Vuorinen, and J.K. Kivilahti, *IEEE Trans. Electron. Packag. Manuf.* 25, 162 (2002).
26. M.O. Alam, Y.C. Chan, and K.N. Tu, *Chem. Mater.* 15, 4340 (2003).
27. H. Yu, V. Vuorinen, and J.K. Kivilahti, *J. Electron. Mater.* 36, 136 (2007).
28. The SGTE databank for solutions and substances, Department of Materials Science and Engineering, The Royal Institute of Technology, Sewden, released 1992.
29. J.-H. Shim, C.-S. Oh, B.-J. Lee, and D.-N. Lee, *Z. Metallkd.* 87, 205 (1996).
30. H.S. Liu, J. Wang, and Z.P. Jin, *Calphad* 28, 363 (2004).
31. K. Rönkä, F.J.J. van Loo, and J.K. Kivilahti, *Scripta Mater.* 37, 1575 (1997).
32. L.S. Darken and R.W. Gurry, *Physical Chemistry of Metals* (McGraw-Hill, 1953).
33. A.T. Dinsdale, *Calphad* 15, 317 (1991).
34. F.J.J. van Loo, *Prog. Solid State Chem.* 20, 47 (1990).
35. E.K. Ohriner, Welding Research Supplement, July 191 (1987).
36. S.-W. Chen, S.-H. Wu, and S.-W. Lee, *J. Electron. Mater.* 32, 1188 (2003).
37. G. Ghosh, *Acta Metall. Mater.* 49, 2609 (2002).

38. G. Ghosh, *J. Electron. Mater.* 33, 229 (2004).
39. T.M. Korhonen, S.J. Hong, P. Su, and M.A. Korhonen, *Proceedinds of the 2000 SMTA International Conference* (Chicago, Illinois, September 24–28, 2000).
40. J. Miettinen, *Calphad* 27, 309 (2003).
41. J.S. Lee Pak and K. Mukherjee, *Mater. Sci. Eng. A Struct.* A117, 167 (1989).
42. H. Yu, V. Vuorinen, and J. K. Kivilahti, *The Proceedings of Electronic Component and Technology Conference, IEEE* (2006).
43. R. Gagliano, G. Ghosh, and M. Fine, *J. Electron. Mater.* 31, 1195 (2002).
44. T. Laurila, V. Vuorinen, and J.K. Kivilahti, *Mater. Sci. Eng. R.* R49, 1 (2005).